

Effect of Nanograss and Annealing Temperature on TiO₂ Nanotubes Based Dye Sensitized Solar Cells

Johns Naduvath^{1, a, *}, Santosh Shaw^{1, b, *}, Parag Bhargava^{1, c}, Sudhanshu Mallick^{1, d}

¹Department of Metallurgical Engineering and Materials Science,

Indian Institute of Technology Bombay, Mumbai-400076, India

^ajohnsnaduvath@iitb.ac.in, ^btosantoshu@gmail.com, ^cpbhargava@iitb.ac.in, ^dmallick@iitb.ac.in

* These authors contributed equally

Keywords: Titanium dioxide Nanotubes; Anodization; Nanograss; Dye sensitized solar cell.

Abstract

In TiO₂ nanoparticle based dye sensitized solar cells (DSSC), the electron injected from the dye has to cross multiple interparticle boundaries in random directions before reaching the electrode. For application in DSSCs, the directional pathway for electron transport through the nanotubes is known to reduce the recombination rate. In the present study, titania nanotubes with nanograss layer have been fabricated by anodization of titanium foil in fluoride containing organic electrolyte. Dye sensitized solar cells with photoanode made of titania nanotubes covered with nanograss was found to have a higher efficiency than ones made with only titania nanotubes of the same length. This can be attributed to enhanced dye adsorption on nanotubes with nanograss. The efficiency of DSSC using titania nanotubes is also affected by the annealing conditions such as duration, temperature.

Introduction

Titanium dioxide (TiO₂) nanostructures have attracted great interest for many applications such as photocatalysis [1], dye sensitized solar cells (DSSC) [2] and electrochemical sensors [3]. The n-type nature, wide bandgap, stability, non-toxicity make TiO₂ suitable for dye sensitized solar cells [4]. In 1991, O'Regan and Gratzel first introduced DSSC as a low cost renewable energy source with potential for large scale production and high efficiency [5]. After that academicians and industrialists have showed extent research interest among in understanding the working principles of DSSC in order to improve the performance of solar cell characteristics. The maximum efficiency achieved in dye sensitized solar cell at AM 1.5 sun light (100mW/cm²) is 12.3% efficiency using TiO₂ nanoparticles [6].

In DSSC, the excited electrons are transferred from the LUMO of dye to the conduction band of the photoanode. For effective transfer of these electrons will happens only the conduction band of the metal oxide should be lower than the LUMO energy level of the dye. The TiO₂ are available in three crystal forms, namely rutile (E_g ≈ 3.05 eV), anatase (E_g ≈ 3.23 eV), and brookite (E_g ≈ 3.26 eV) [7]. Rutile is the most common and stable TiO₂ polymorph. But anatase is the preferred structure in DSSC due to its large band gap and higher conduction band edge energy. The photocurrent of DSSC using rutile TiO₂ was about 30% lesser than that of the anatase because of its lower surface area which affects dye loading [8].

The nanotubes and nanorods with special geometry have high surface area and aspect ratio which are highly desirable for its applications like dye sensitized solar cells, gas sensors, photocatalysis etc [9]. Titanium dioxide with different morphology can be synthesized using hydrothermal process [10], sol-gel method [11], and alumina template method [12]. Electrochemical etching or controlled anodization of titanium (Ti) in fluoride ions containing electrolytes are well established method for the fabrication of highly ordered vertically oriented nanotube arrays [13]. Maggie Paulose et al. in 2006 fabricated back illuminated DSSC with 4.24% efficiency using N719 sensitized TiO_2 nanotube [14]. Kim et al. reported that the presence of TiO_2 nanograss decreasing the photocurrents and conversion efficiencies of DSSC [15]. In this paper, we investigated the effect of nanograss with respect to anodization voltage. The influences of dye loading on photovoltaic properties of DSSC made using TiO_2 nanotubes with nanograss layer at different length were also investigated. The properties of DSSC using TiO_2 nanotubes annealed at different temperature ranges and durations were studied.

Experimental Details

Synthesis of TiO_2 nanotubes and nanograss.

Titanium foils (0.6 mm thick, $\geq 99.2\%$, TIMET, grade 2) of 2.0 cm x 1.5 cm dimension were cleaned by sonicating in acetone, methylene chloride and ethanol for 10 minutes respectively, rinsed with deionized (DI) water and dried in air. Anodization was carried out using a locally made two electrode setup with Ti foil of size 2x2 cm as counter electrode and voltage was applied by a DC power supply (Aplab limited, Mumbai). Highly ordered TiO_2 nanotube arrays were fabricated by anodic oxidation of Ti foil at various steady state potentials (15 V – 75 V) attained with a ramp rate of 5 V min^{-1} in 0.5 wt% NH_4F and 2 vol% H_2O containing ethylene glycol solution. After 1-6 hours of anodization, the films were cleaned thoroughly using DI water and dried using hot air blower. The films were ultrasonicated in DI water for 1 minute to remove the nanograss present on the surface of the TiO_2 nanotube film.

Annealing of TiO_2 nanotubes

For annealing of as-formed (amorphous) nanostructures, furnace temperature was ramped at 1°C min^{-1} to 200°C , held for 1 hour, and then ramped to 450 and 500°C , held for 3 and 6 hours to induce crystallinity and to remove organic residues. Annealed samples were taken out for dye adsorption when temperature was around 120°C .

Fabrication of dye sensitized solar cells

Annealed nanotube layers (both with and without nanograss layer) were sensitized with dye by soaking in a 0.3 mM *cis*-bis(isothiocyanato)bis(2,2'-bipyridyl-4,4'-dicarboxylato)-ruthenium(II) (N_3)(Dyesol) dye solution in ethanol for 24 hours. Fluorine doped tin oxide (FTO) substrate (TEC8, sheet resistance 8-9 Ω/\square Pilkington) coated with platinum by thermal decomposition of H_2PtCl_6 (Thomas Baker) solution in isopropyl alcohol, was used as the counter electrode. The dye loaded

TiO₂ photoanodes and thermally deposited Pt counter-electrodes were assembled in a sandwich-type cell with the help of supporting clamps, using a 60 µm thick Surlyn (SX1170-60PF, Solaronix) spacer in between to contain the electrolyte solution made from 0.1 M LiI (LR, Thomas Baker), 0.05 M I₂ (LR, Thomas Baker) and 0.5 M 4-tert-butylpyridine (Sigma Aldrich - 96%) dissolved in acetonitrile.

Characterization

Morphology of the nanostructured oxide layers were characterized using HITACHI S-3400N Scanning Electron Microscope (SEM) and JEOL JSM 7600F Field Emission Scanning Electron Microscope (FE-SEM). The photocurrent-photovoltage (I-V) characteristics was measured under AM 1.5G (Newport Solar Class A Solar Simulator) with intensity of 100 mWcm⁻² (measured by Newport power meter) using a Keithley 2420 High-Current Source Meter. UV-Spectroscopy (Jasco V-650 spectrophotometer with Spectra Manager software) was utilized to measure the dye loading of the photoanodes and diffused reflectance spectra of TiO₂ nanotube with and without nanograss.

The key characteristics of a solar cell are short circuit current density (J_{sc}), the open circuit voltage (V_{oc}), efficiency (η) and the fill factor (FF). They are related to each other as follows [16]:

$$\eta = \frac{J_{sc} \times V_{oc} \times FF}{I_p} \quad (1)$$

$$FF = \frac{J_{max} \times V_{max}}{J_{sc} \times V_{oc}} \quad (2)$$

where J_{max} , V_{max} , are the corresponding current density and voltage values where the solar cell delivers maximum power and I_p is the illuminated light intensity (100 mWcm⁻²).

Results and Discussion

Effect of nanograss in dye sensitized solar cell

During electrochemical anodization, the oxygen ions from water interact with Ti metal and form an oxide layer. Due to high electric field Ti⁴⁺ metal ion migrated from the metal/oxide interface and metal/electrolyte interface and causes field assisted dissolution. Along with field assisted dissolution, presence of F⁻ ions causes chemical dissolution and form porous structure on the TiO₂ thin film [16]. A layer of nanograss was formed over the TiO₂ nanotubes during the anodization using electrolyte containing 0.5 wt% NH₄F and 2 vol% H₂O in ethylene glycol at 55 V for 4 hour (Fig. 1(a) and 1(c)). The nanograss is formed due to vertical splitting top of the tubes because of the excessive etching [17]. Sonication for 60 seconds in DI water results in removal of the nanograss layer, exposing the underlying open nanotubes (Fig. 1(b) and 1(d)).

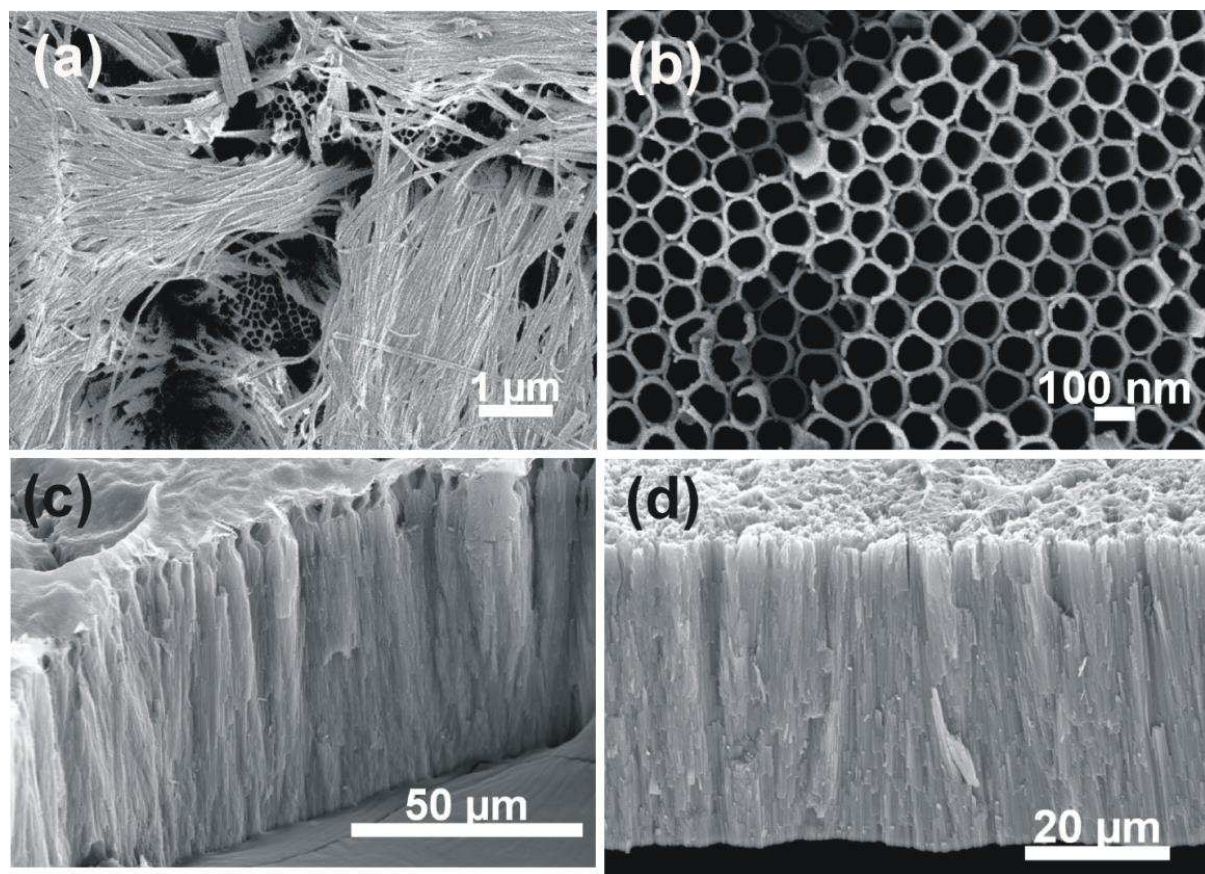


Fig .1. (a) and (c) Top & cross sectional views of anodized film before sonication (b) and (d) Top & cross sectional views of film after sonication.

The effect of anodization voltage on the extent of nanoglass growth was evaluated by carrying out the anodization at various voltages, ranging from 75 V to 15 V, keeping the water content in electrolyte at 2 vol%. As seen from figure 2, the extent of nanoglass formation increases with anodization voltage. It is also noticed the nanotube inner diameter increased from ~30 nm to ~155 nm as the anodization voltage was varied from 15 V to 75 V.

At high anodization voltage, there is an increase in the potential difference across the oxide-electrolyte and metal-oxide interfaces. The electric field causes polarization of Ti–O bond in TiO_2 forming Ti^{4+} and O^{2-} ions. The Ti^{4+} ions dissolve in the electrolyte, promoting field assisted dissolution of the metal oxide [16]. This dissolution eventually aids in the thinning of the tube top that leads to vertical splitting due to viscous forces and results in the formation of nanoglass.

X-Ray diffraction of annealed TiO_2 nanotubes (Fig. 2) shows predominantly anatase phase (as per JCPDS 01-084-1285). The XRD data was normalized with respect to the highest intensity peak (101). A comparison with Degussa P25 powder XRD shows a significant difference in the (004) peak intensity suggesting a preferential growth of nanotube and nanoglass along that direction.

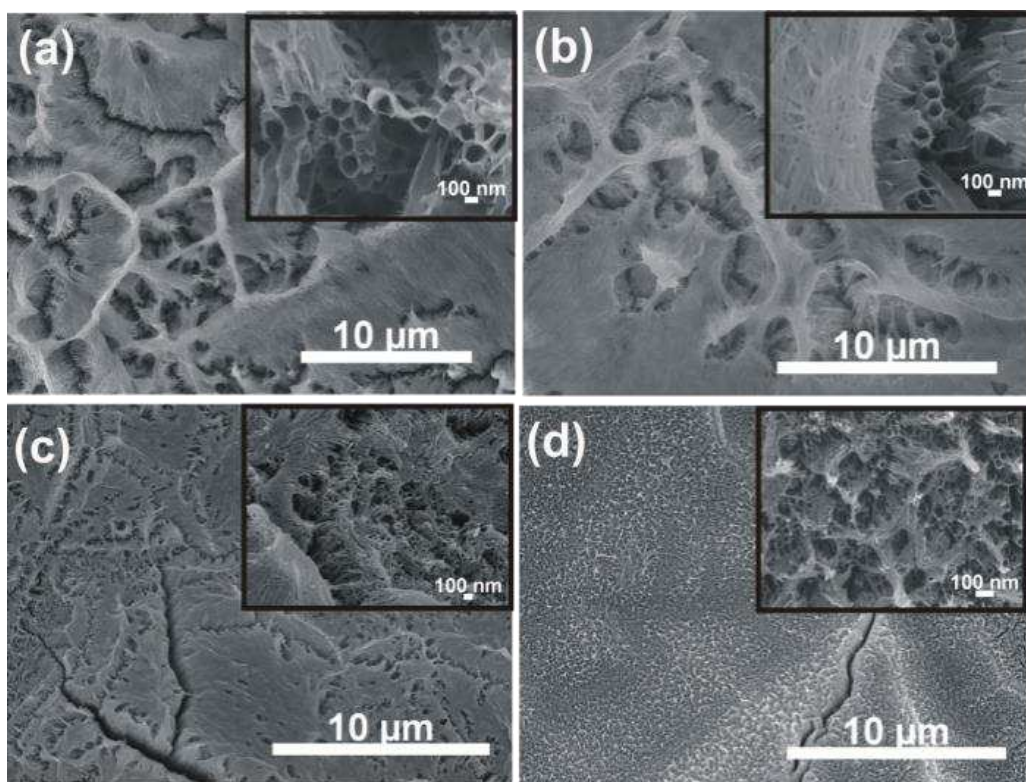


Fig.2. SEM images of the TiO_2 layer anodized at different voltages (a) 75 V (b) 55 V (c) 25 V and (d) 15 V with inset showing images at higher magnification.

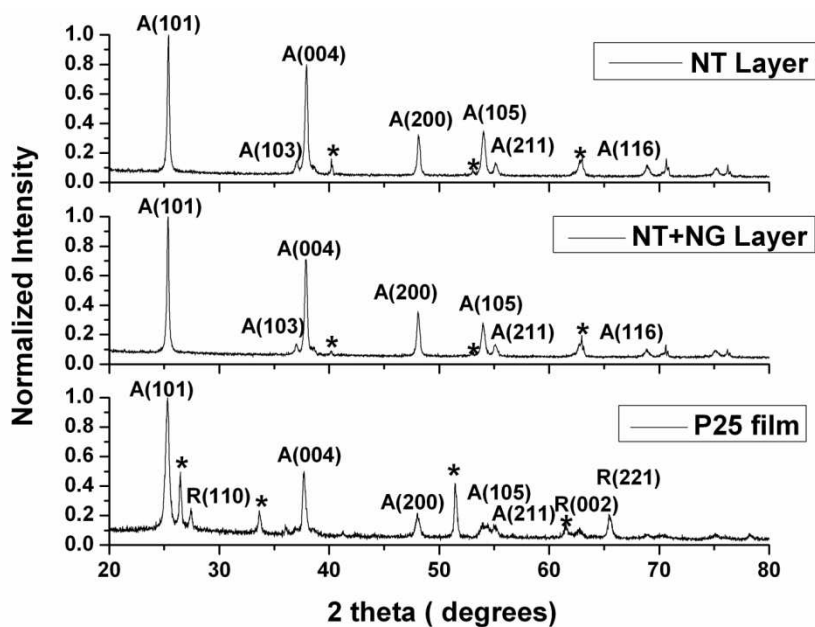


Fig.3. XRD of titania nanotubes annealed at 500°C for 6 hours with nanograss layer (NT+NG), without nanograss (NT) and Degussa P25 film. “A” is Anatase. “*” is substrate (Ti substrate for nanotube and FTO for P25 powder).

In order to study the effect of nanograss layer on the dye sensitized solar cell performance, TiO₂ nanotubes layers of different length were grown by varying the anodization time from 1 hour to 6 hours while keeping the anodization voltage constant at 55V and water content at 2 vol%. Figure 4 shows the comparison of dye loading and photovoltaic characteristics (η , J_{sc} , V_{oc}) of cells made from as-anodized (NT+NG) with that of sonicated (NT) photoanode of different nanotube lengths. Active area of the solar cell was approximately 0.4 cm² and light intensity was maintained at 100 mWcm⁻² (AM 1.5).

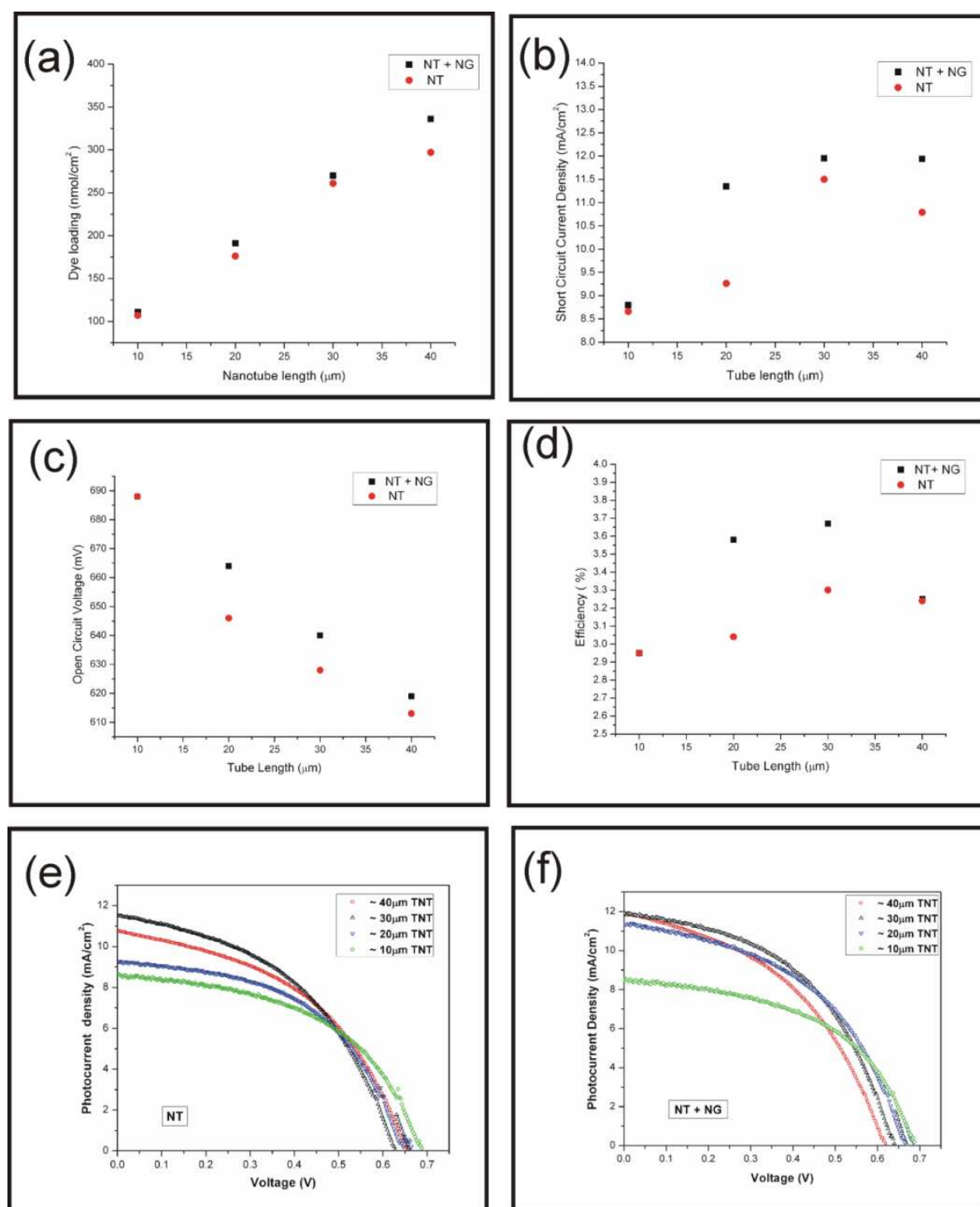


Fig. 4. Photovoltaic performance of solar cells made from photoanodes with nanograss (NT+NG) and without nanograss (NT).

Figure 4(b) shows that as the length increases, short circuit current density (J_{sc}) increases, reaches a maximum, and decreases gradually for longer tube lengths. The surface area and the dye loading increases with increasing tube length. However, after an optimum length, the recombination of the photogenerated electrons with the electrolyte increases, reducing the short circuit current. The larger surface area of the as-anodized nanotubes with nanograss layer results in a 3-13% higher dye loading and higher photocurrent density in comparison to just the nanotube layer (Fig.4(a)).

Figure 4(c) shows that open circuit potential (V_{oc}) decreases with increasing nanotube length. The V_{oc} in a dye sensitized solar cell is defined as the difference between the Fermi level of TiO_2 and the redox potential of I^-/I_3^- pair in the electrolyte. The decrease of V_{oc} with the increasing tube length in this work is a consequence of high recombination events at the surface of the nanotube during the diffusion of the electrons injected from the dye. Higher series resistance of longer titania tubes also contributes to a reduction in the V_{oc} .

The V_{oc} of DSSC made using nanotube with nanograss is larger than those made from nanotube free of nanograss. In order to study this phenomenon, the band gap of both films was calculated from UV-Vis spectroscopy (Fig. 5). These correspond to a band gap of 3.0 eV for nanotube layer and 3.2 eV for nanotube layer with nanograss. This possibly results in different Fermi energies and consequently difference in the V_{oc} [18].

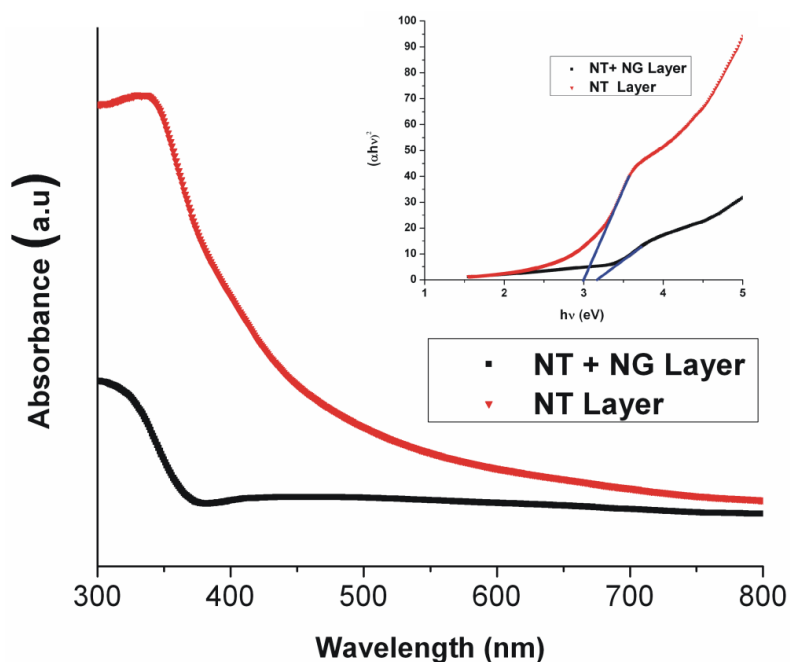


Fig. 5. Diffuse reflectance UV-Visible spectra of TiO_2 nanotube with and without nanograss with inset showing the bandgap calculation.

Though the variation of J_{sc} and V_{oc} with tube length was opposite to each other, the improvement in the overall conversion efficiency (η) is evident up to a critical titania tube length (Fig. 4(d)). Above this optimal tube length, recombination becomes prominent reducing the power conversion efficiency. The optimum nanotube length was found to be 30 μm where the solar cell has the highest efficiency (3.67%).

Effect of annealing temperature of TiO₂ nanotubes in dye sensitized solar cell

In order to study the effect of annealing temperature on TiO₂ nanotubes on dye sensitized solar cell, the TiO₂ nanotubes was annealed at different temperatures for different durations. Figure 6 shows X-ray diffraction spectra taken for the as anodized nanotubes annealed in air at different conditions. X-ray diffraction analysis shows that as anodized TiO₂ films to be amorphous in nature at room temperature (Fig. 6a). From the XRD spectra, it was found that crystallization of TiO₂ nanotubes starts at temperature between 200 to 300°C and it crystallization increases into more of anatase phase at high temperatures (Here we consider only anatase (004) plane). At 450°C for 3 hours, TiO₂ nanotube shows polycrystalline nature. The peaks at 25.3°, 37.8°, 48.0°, 53.9° and 54.6° represents (101), (004), (200), (105) and (211) planes of anatase TiO₂ (Fig. 6b). The XRD data was normalized with respect to the highest intensity peak (101). As temperature increases, the intensity of (004) peak is also increasing. This implies (004) oriented growth of crystallites inside the tubes of TiO₂ crystals.

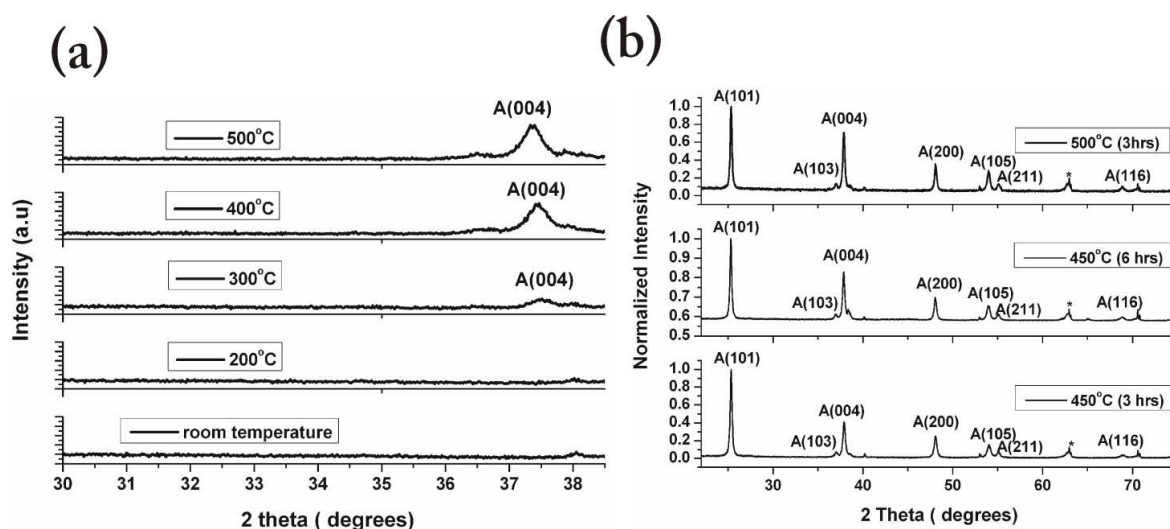


Fig.6. XRD of titania nanotubes annealed at different temperatures and durations. “A” is Anatase. “*” is Ti substrate.

It is clear that with increase in annealing temperature, increases the amount of conversion of sample to anatase phase which directly relates to the increase in photocurrent (Fig. 7). It is also found that increase in annealing time, there is markedly increase in photocurrent. This can be probably due to the increase in crystallite size in tube wall with annealing time, which decreases the effective phase boundary area for electron transfer. It is known that phase boundary has deleterious effect on electron pathway which ultimately leads to recombination. So growth of crystallite in (004) orientation increases the photocurrent. Overall, annealing temperature and annealing duration has impact on the photovoltaic performance.

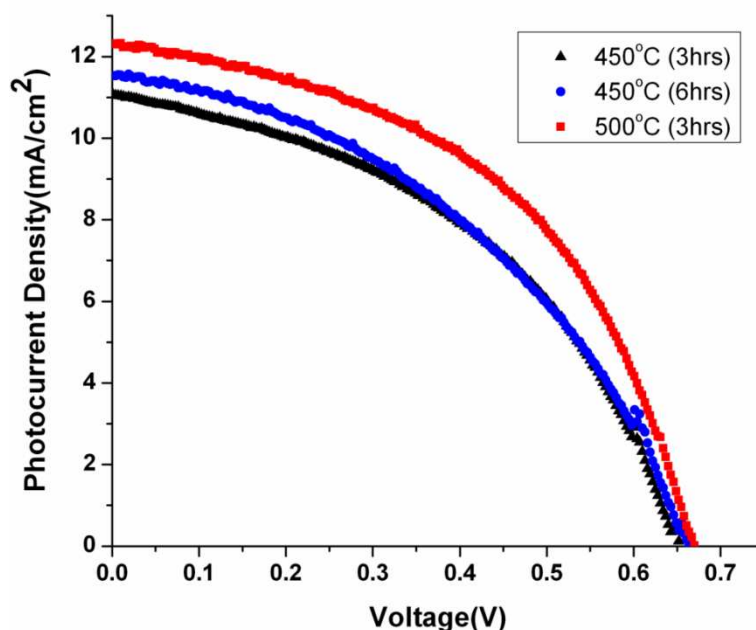


Fig. 7. I-V curve of cell using TiO_2 nanotube only at different annealing conditions. Electrode thickness for all cells was $\sim 30\mu\text{m}$.

Summary

It was observed that the anodization of Ti foil above 40V leads to the formation of nanograss over TiO_2 nanotubes. Presence of nanograss layer on the titania nanotube improves the dye loading of the sample compared with nanotube without nanograss causing increment in the photocurrent in DSSCs in the former case. Because of increased bandgap, the photovoltage of DSSC made of nanograss is also increased. The preferential growth of crystallites in (004) orientation during annealing also contributed towards increase in the photocurrent of DSSC made up of TiO_2 nanotubes.

Acknowledgment

The authors would like to acknowledge NCPRE (National Center for Photovoltaic Research and Education), SAIF (Sophisticated Analytical Instrument Facility) and the Department of Metallurgical Engineering and Materials Science, Indian Institute of Technology Bombay, for the experimental and analytical facilities. The authors would also like to acknowledge Dr. Jaykrushna Das, Ajay Kumar Jena and Shyama Prasad Mohanty, Pragyensh Kumar, for technical discussions.

References

- [1] A. Fujishima, T. N. Rao, D. A. Tryk, Titanium dioxide photocatalysis, *J. Photochem. Photobiol. C. Photochem. Rev.* 1 (2000) 1–21.
- [2] M. Gratzel, Photoelectrochemical cells, *Nature*. 414 (2001) 338–344.
- [3] O.K. Varghese, D. Gong, M. Paulose, K. G. Ong, C. A. Grimes, Hydrogen sensing using titania nanotubes, *Sens. Actuators B*. 93 (2003) 338–344.
- [4] A. Hagfeldt, G. Boschloo, L. Sun, L. Kloo, H. Pettersson, Dye-sensitized solar cell, *Chem. Rev.* 110 (2010) 6595–6663.
- [5] B.O. Regan, M. Gratzel, A low-cost, high-efficiency solar cell based on dye-sensitized colloidal TiO₂ films, *Nature*. 353 (1991) 737–740.
- [6] A. Yella, H. Lee, H. N. Tsao, C. Yi, A. K. Chandiran, M. K. Nazeeruddin, E. W. Diau, C. Yeh, S. M. Zakeeruddin, M. Grätzel, Porphyrin-sensitized solar cells with Cobalt (ii/iii)–based redox electrolyte exceed 12 percent efficiency, *Science*, 334 (2011) 629–634.
- [7] R. Jose, V. Thavasi, S. Ramakrishna. Metal oxides for dye sensitized solar cells, *J. Am. Ceram. Soc.* 92, 2 (2009) 289–301.
- [8] N.-G. Park, J. van de Lagemaat, A. J. Frank, Comparison of dye sensitized rutile and anatase-based TiO₂ solar cells, *J. Phys. Chem. B*. 104 (2000) 8989–8994.
- [9] P. Roy, S. Berger, P. Schmuki, TiO₂ nanotubes: Synthesis and applications. *Angew. Chem. Int. Ed.* 50 (2011) 2904–2939.
- [10] D. V. Bavykin, V. N. Parmon, A. A. Lapkin, F. C. Walsh, The effect of hydrothermal conditions on the mesoporous structure of TiO₂ nanotubes. *J. Mater. Chem.* 14 (2004) 3370–3377.
- [11] T. Kasuga, M. Hiramatsu, A. Hoson, T. Sekino, K. Niihara, Formation of Titanium Oxide nanotube. *Langmuir*, 14 (1998) 3160–3163.
- [12] M. S. Sander, M. J. Cote, W. Gu, B. M. Kile, C.P. Tripp, Template-assisted fabrication of dense, aligned arrays of titania nanotubes with well controlled dimensions on substrates. *Adv. Mater.* 16 (2004) 2052–2057.
- [13] D. Gong, C. A. Grimes, O. K. Varghese, W. Hu, R. S. Singh, Z. Chen, E. C. Dickey, Titanium oxide nanotube arrays prepared by anodic oxidation. *J. Mater. Res.* 16 (2001) 3331–3334.
- [14] M. Paulose, K. Shankar, O. K. Varghese, G. K. Mor, B. Hardin and C. A. Grimes, Backside illuminated dye sensitized solar cells based on titania nanotube array electrodes, *Nanotechnology* 17 (2006) 1446–1448.

-
- [15] D. Kim, A. Ghicov, P. Schmuki, TiO₂ Nanotube arrays: Elimination of disordered top layers (“nanograss”) for improved photoconversion efficiency in dye-sensitized solar cells, *Electrochem. Commun.* 10 (2008) 1835–1838.
- [16] C. A. Grimes, G. K. Mor, TiO₂ nanotube arrays synthesis, properties, and applications, Springer, 2009.
- [17] J. H. Lim, J. Choi, Titanium Oxide nanowires originating from anodically grown nanotubes: the Bamboo splitting model, *Small*. 3 (2007) 1504 –1507.
- [18] Z. Sun, J. H. Kim, T. Liao, Y. Zhao, F. Bijarbooneh, V. Malgras, S. X. Dou, Continually adjustable oriented 1DTiO₂ nanostructure arrays with controlled growth of morphology and their application in dyesensitized solar cells. *CrysEngComm*. 14 (2012) 5472–5478.

Potential Development in Dye-Sensitized Solar Cells for Renewable Energy

10.4028/www.scientific.net/MSF.771

Effect of Nanograss and Annealing Temperature on TiO₂ Nanotubes Based Dye Sensitized Solar Cells

10.4028/www.scientific.net/MSF.771.103

DOI References

[1] A. Fujishima, T. N. Rao, D. A. Tryk, Titanium dioxide photocatalysis, J. Photochem. Photobiol. C. Photochem. Rev. 1 (2000) 1–21.

[http://dx.doi.org/10.1016/S1389-5567\(00\)00002-2](http://dx.doi.org/10.1016/S1389-5567(00)00002-2)

[2] M. Gratzel, Photoelectrochemical cells, Nature. 414 (2001) 338-344.

<http://dx.doi.org/10.1038/35104607>

[3] O.K. Varghese, D. Gong, M. Paulose, K. G. Ong, C. A. Grimes, Hydrogen sensing using titania nanotubes, Sens. Actuators B. 93 (2003) 338–344.

[http://dx.doi.org/10.1016/S0925-4005\(03\)00222-3](http://dx.doi.org/10.1016/S0925-4005(03)00222-3)

[4] A. Hagfeldt, G. Boschloo, L. Sun, L. Kloo, H. Pettersson, Dye-sensitized solar cell, Chem. Rev. 110 (2010) 6595–6663.

<http://dx.doi.org/10.1021/cr900356p>

[5] B.O. Regan, M. Gratzel, A low-cost, high-efficiency solar cell based on dye-sensitized colloidal TiO₂ films, Nature. 353 (1991) 737- 740.

<http://dx.doi.org/10.1038/353737a0>

[14] M. Paulose, K. Shankar, O. K. Varghese, G. K Mor, B. Hardin and C. A Grimes, Backside illuminated dyesensitized solar cells based on titania nanotube array electrodes, Nanotechnology 17 (2006) 1446–1448.

<http://dx.doi.org/10.1088/0957-4484/17/5/046>